Submitted to Physics Letters B

LBL-1921
Preprint c.1

PAIRING AND SPIN DISTRIBUTION EFFECTS ON THE YRAST LINE

RECEIVED
LAWRENCE
RADIATION LABORATORY

JUL 25 1973

LIBRARY AND
DOCUMENTS SECTION

L. G. Moretto

June 1973

Prepared for the U. S. Atomic Energy Commission
under Contract W-7405-ENG-48

For Reference

Not to be taken from this room

LAWRENCE BERKELEY LABORATORY
UNIVERSITY OF CALIFORNIA
BERKELEY

LBL-1921
c.1

DISCLAIMER

This document was prepared as an account of work sponsored by the United States Government. While this document is believed to contain correct information, neither the United States Government nor any agency thereof, nor the Regents of the University of California, nor any of their employees, makes any warranty, express or implied, or assumes any legal responsibility for the accuracy, completeness, or usefulness of any information, apparatus, product, or process disclosed, or represents that its use would not infringe privately owned rights. Reference herein to any specific commercial product, process, or service by its trade name, trademark, manufacturer, or otherwise, does not necessarily constitute or imply its endorsement, recommendation, or favoring by the United States Government or any agency thereof, or the Regents of the University of California. The views and opinions of authors expressed herein do not necessarily state or reflect those of the United States Government or any agency thereof or the Regents of the University of California.

0 0 0 0 5 9 0 0 5 5 7

PAIRING AND SPIN DISTRIBUTION EFFECTS ON THE YRAST LINE*

L. G. Moretto

Department of Chemistry and
Lawrence Berkeley Laboratory
University of California
Berkeley, California 94720

June 1973

The shape of the yrast line in the paired region is studied on the basis of the uniform model and of two extreme spin projection distributions. It is shown that the form of the yrast line depends strongly upon the assumed spin projection distribution.

— — —

The superfluid properties of nuclei are best established in the ground state. In turn the angular momentum is known to attenuate and eventually destroy the pairing correlation. Therefore the interaction between pairing and angular momentum should be best observed along the yrast line, namely along the locus of the lowest energy levels at the various angular momenta.

Some anomalies in the rotational bands of deformed nuclei[1] have been attributed to the disappearance of pairing with increasing angular momentum.[2] Such effects should be more pronounced and more easily understood in spherical nuclei. In these nuclei the effective moment of inertia is more sensitive to pairing. In fact the moment of inertia of any object tends towards its rigid value with increasing deformation independently from the flow of matter.

The detailed shape of the yrast line depends also upon the local fluctuations of spacings and spins occurring at the Fermi surface. In order

*Work performed under the auspices of the U. S. Atomic Energy Commission.

to single out the features which are associated with the angular momentum and pairing interaction, the shell effects can be eliminated by using a uniform model where the level spacing is constant. In this case the yrast line, for a spherical nucleus, is completely determined by the pairing strength G, by the density g of the doubly degenerate single particle levels and by the distribution of the single particle spin projections p(m). It will be shown that the spin projection distribution is most important in determining both the slope and the curvature of the yrast line. In the present study two extreme spin projection distributions are used. The first is a δ function: $p(m) = \delta(m - \underline{m})$. The second is a rectangular distribution: $p(m) = \text{constant for } 0 \leqslant m \leqslant m_x$ and $p(m) = 0$ for $m > m_x$, m_x being the largest possible spin projection.

Three equations are needed to study the overall behavior of the yrast line. The gap equation:

$$\sum \frac{1}{2E_k} \left[\tanh \frac{1}{2} \beta(E_k - \gamma m_k) + \tanh \frac{1}{2} \beta(E_k + \gamma m_k)\right] = \frac{2}{G} \quad . \tag{1}$$

The angular momentum equation:

$$I = \sum m_k \left[\frac{1}{1 + \exp \beta(E_k - \gamma m_k)} - \frac{1}{1 + \exp \beta(E_k + \gamma m_k)} \right] \quad . \tag{2}$$

The energy equation:

$$E = \sum \varepsilon_k \left[1 - \frac{\varepsilon_k - \lambda}{2E_k} \left\{ \tanh \frac{1}{2} \beta(E_k - \gamma m_k) + \tanh \frac{1}{2} \beta(E_k + \gamma m_k) \right\} \right] - \frac{\Delta^2}{G} \quad . \tag{3}$$

In these equations ε_k and m_k are the single particle energies and spin projections respectively; $E_k = [(\varepsilon_k - \lambda)^2 + \Delta^2]^{1/2}$; Δ is the gap parameter; λ is the chemical potential which, for the uniform model, is a constant and can

be set equal to zero; γ is the angular velocity of the nucleus. The above equations describe the yrast line when $\beta \to \infty$.

The first spin projection distribution $p(m) = \delta(m - \underline{m})$ has been applied before to eq. (1), eq. (2), and eq. (3) with the following results:[3]

$I \leqslant I_{cr}$	$I \geqslant I_{cr}$	
$\frac{\Delta}{\Delta_o} = \left(1 - \frac{I}{I_{cr}}\right)^{1/2}$	$\Delta = 0$	(4)
$\gamma = \frac{I_{cr}}{\mathfrak{J}_R}\left(2 - \frac{I}{I_{cr}}\right)$	$\gamma = \frac{I}{\mathfrak{J}_R}$	(5)
$\mathfrak{J} = \mathfrak{J}_R \frac{I/I_{cr}}{2 - I/I_{cr}}$	$\mathfrak{J} = \mathfrak{J}_R$	(6)
$E_y = \frac{I_{cr}^2}{\mathfrak{J}_R} \frac{I}{I_{cr}}\left(2 - \frac{I}{2I_{cr}}\right)$	$E_y = \frac{I_{cr}^2}{\mathfrak{J}_R} + \frac{I^2}{2\mathfrak{J}_R}$	(7)

where Δ_o is the ground state gap parameter, $\mathfrak{J}$ is the moment of inertia and E_y is the yrast energy. The critical angular momentum I_{cr} where pairing disappears is given by: $I_{cr} = \underline{m}g\,\Delta_o$ and the rigid moment of inertia $\mathfrak{J}_R$ is given by $\mathfrak{J}_R = 2\,\underline{m}^2 g$. The dependence of the angular velocity γ, of the moment of inertia $\mathfrak{J}$ and of the yrast energy E_y, upon the angular momentum I is shown by means of thin lines in figs. 1, 2, and 3. From eq. (5) and fig. 1 it is seen that, below the critical angular momentum, γ is a decreasing function of I. This is immediately reflected upon the shape of the yrast line since $\gamma = \frac{dE}{dI}$. Thus it can be seen from eq. (7) and fig. 3 that the yrast line below the critical angular momentum is characterized by a negative second derivative. This can be understood qualitatively as follows. Every broken pair generates two

quasi-particles which, because of the constant spin projections, contribute always the same amount of angular momentum. Thus the angular momentum is proportional to the number of quasi-particles. On the other hand the energy cost of two quasi-particles decreases with the number of quasi-particles already present, because of the blocking effects. Therefore the energy will increase less and less as the angular momentum increases.

The second spin projection distribution $p(m)$ = constant for $m \leqslant m_x$ $p(m) = 0$ for $m > m_x$ does not lead to an equivalently elegant analytical formalism. However it is very interesting because it closely simulates the case of a spherical nucleus where the Fermi surface is sampling all the $2J + 1$ spin projections of a given J shell.

The angular momentum equation can be integrated analytically and yields:

$$I = \frac{2}{3} \frac{g}{\gamma^2 m_x} [\gamma^2 m_x^2 - \Delta^2]^{3/2} \quad . \tag{8}$$

Similarly the gap equation becomes:

$$\frac{1}{2} \frac{\gamma m_x}{\Delta^2 \Delta_o} \left\{ (\Delta^2 + \Delta_o^2) \left(1 - \frac{\Delta^2}{\gamma^2 m_x^2}\right)^{1/2} - (\Delta_o^2 - \Delta^2) \right\} = \sinh \left(1 - \frac{\Delta^2}{\gamma^2 m_x^2}\right)^{1/2} \tag{9}$$

These two equations define the two functions $\Delta = \Delta(I)$ and $\gamma = \gamma(I)$. Unfortunately these two functions cannot be expressed analytically. However, it is feasible to calculate the value of γ at $I = 0$ ($\Delta = \Delta_o$) and at $I = I_{cr}$ ($\Delta = 0$):

$$\gamma_{I=0} = \frac{\Delta_o}{m_x} \quad ; \qquad \gamma_{cr} = \frac{e}{2} \frac{\Delta_o}{m_x} \quad , \tag{10}$$

where e is the base of the natural logarithms. We can see immediately that, contrary to the previous case, the angular velocity γ increases in going from $I = 0$ to $I = I_{cr}$. Such an increase is monotonic as shown in fig. 1 by the thick solid curve. The critical angular momentum is given by the relation:

$$I_{cr} = \frac{e}{3} g\, m_x\, \Delta_o \quad . \tag{11}$$

The moment of inertia as a function of angular momentum is shown in fig. 2 by the thick solid curve. Its rigid value, assumed when $I = I_{cr}$ is:

$$\mathfrak{J}_R = \frac{2}{3} g\, m_x^2 \quad . \tag{12}$$

By comparing the two models at constant gap parameter Δ_o and at constant rigid moment of inertia it appears that the rectangular distribution predicts a larger critical angular momentum then the δ distribution:

$$\frac{I_{cr}^{(2)}}{I_{cr}^{(1)}} = \frac{e}{\sqrt{3}} \quad . \tag{13}$$

From eq. (10) and fig. 3 and remembering that $\gamma = \frac{dE}{dI}$ it is concluded that the yrast line should be characterized by a positive second derivative in the paired region. This is in contrast with the previous model which predicts a negative second derivative for the yrast line.

The yrast energy at the critical angular momentum can be calculated directly:

$$E_{y_{I=I_{cr}}} = \frac{1}{2} g\, \Delta_o^2 + \frac{I_{cr}^2}{2\mathfrak{J}_R} = \frac{1}{2} g\, \Delta_o^2 \left(1 + \frac{e^2}{6}\right) \simeq 2.23\, E_{cond} \quad , \tag{14}$$

where $E_{cond} = \frac{1}{2} g \Delta_o^2$ is the condensation energy due to the pairing correlation. It is interesting to note that the previous model predicts $E_{y_{I=I_{cr}}} = 1.5\ E_{cond}$.

The complete yrast line is shown in fig. 3 by the thick solid curve and it does indeed show a slightly positive second derivative in the paired region.

The reason for such a behavior can be qualitatively understood as follows. The first two quasi-particles which are produced occupy the highest portion of the spin projection distribution, generating a certain amount of angular momentum. The next quasi-particles must occupy a lower portion of the spin projection distribution, thus generating less angular momentum per quasi-particle. In other words as the angular momentum increases it takes more quasi-particles to generate a fixed amount of angular momentum. This is in contrast with the previous model where the same number of quasi-particles always produces the same amount of angular momentum. Because of this effect, the flaring out of the previous yrast line is more than compensated by the extra energy needed to produce the extra number of quasi-particles.

It is interesting to realize that a decreasing angular velocity as a function of angular momentum with the consequent negative second derivative of the yrast line is responsible for a back bending in the plot of the moment of inertia versus the square of the angular velocity. It has been shown here that such a back bending depends critically upon the spin projection distribution. A systematic study of these features of the yrast lines should provide a strong test for our understanding of the pairing interaction in nuclei.

References

1. A. Johnson, H. Ryde, and S. A. Hjorth, Nucl. Phys. A179 (1972) 753.
2. J. Krumlinde and Z. Szymanski, Phys. Letters 36B (1971) 157.
3. L. G. Moretto, to be published in Phys. Letters; L. G. Moretto, Nucl. Phys. A185 (1972) 145.

Figure Captions

Fig. 1. Dependence of the angular velocity upon the angular momentum for a δ function spin projection distribution (upper thin line) and for a rectangular spin projection distribution (thick line). The two calculations are normalized to the same critical angular momentum I_{cr}.

Fig. 2. Moment of inertia as a function of angular momentum. The thin and thick lines refer to the two different models as in fig. 1.

Fig. 3. Yrast line for the two models as indicated in fig. 1. The two calculations are normalized to reproduce the same rigid moment of inertia and the same condensation energy. The dashed line merging first into the thin and later into the thick solid line is a parabola corresponding to the yrast line for the unpaired system.

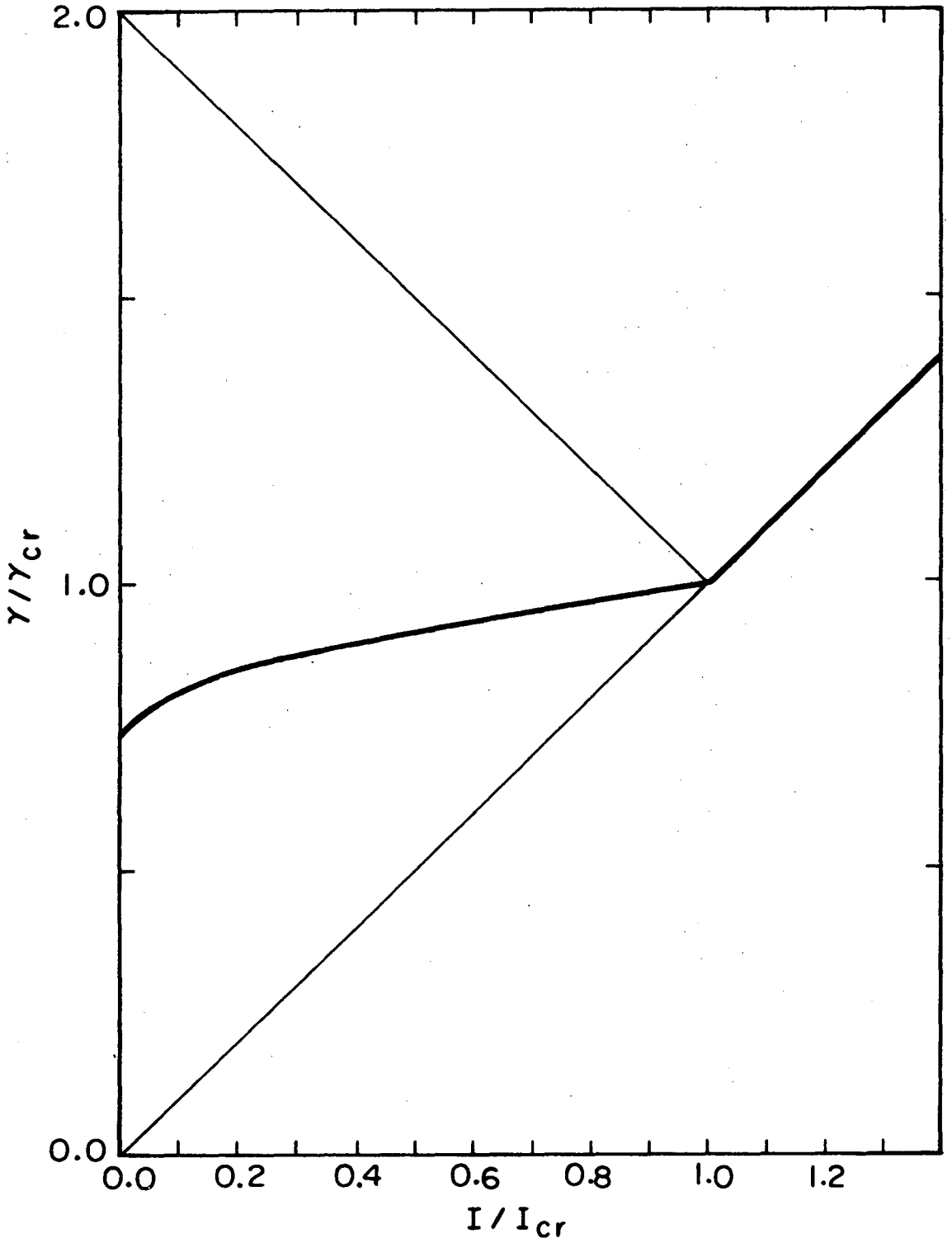

XBL735-2831

Fig. 1

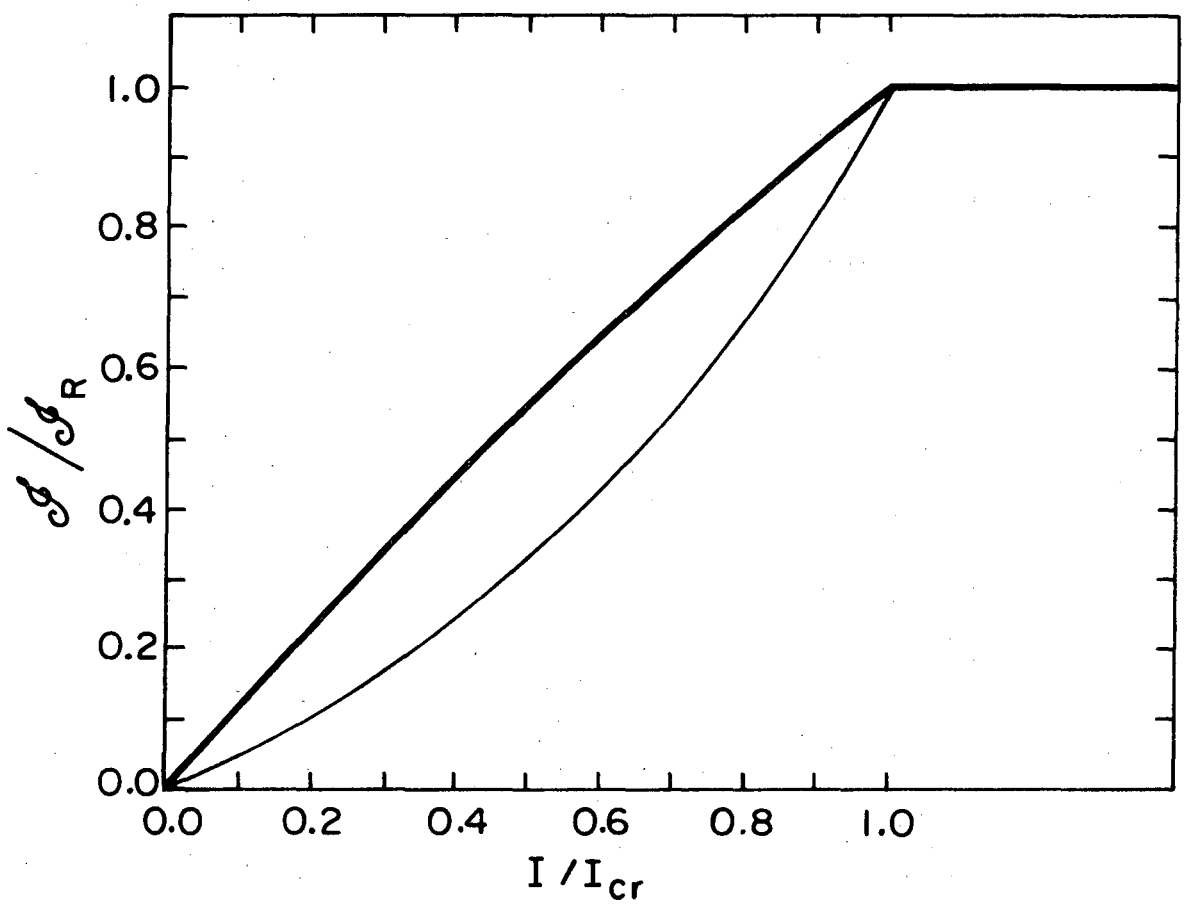

XBL735-2834

Fig. 2

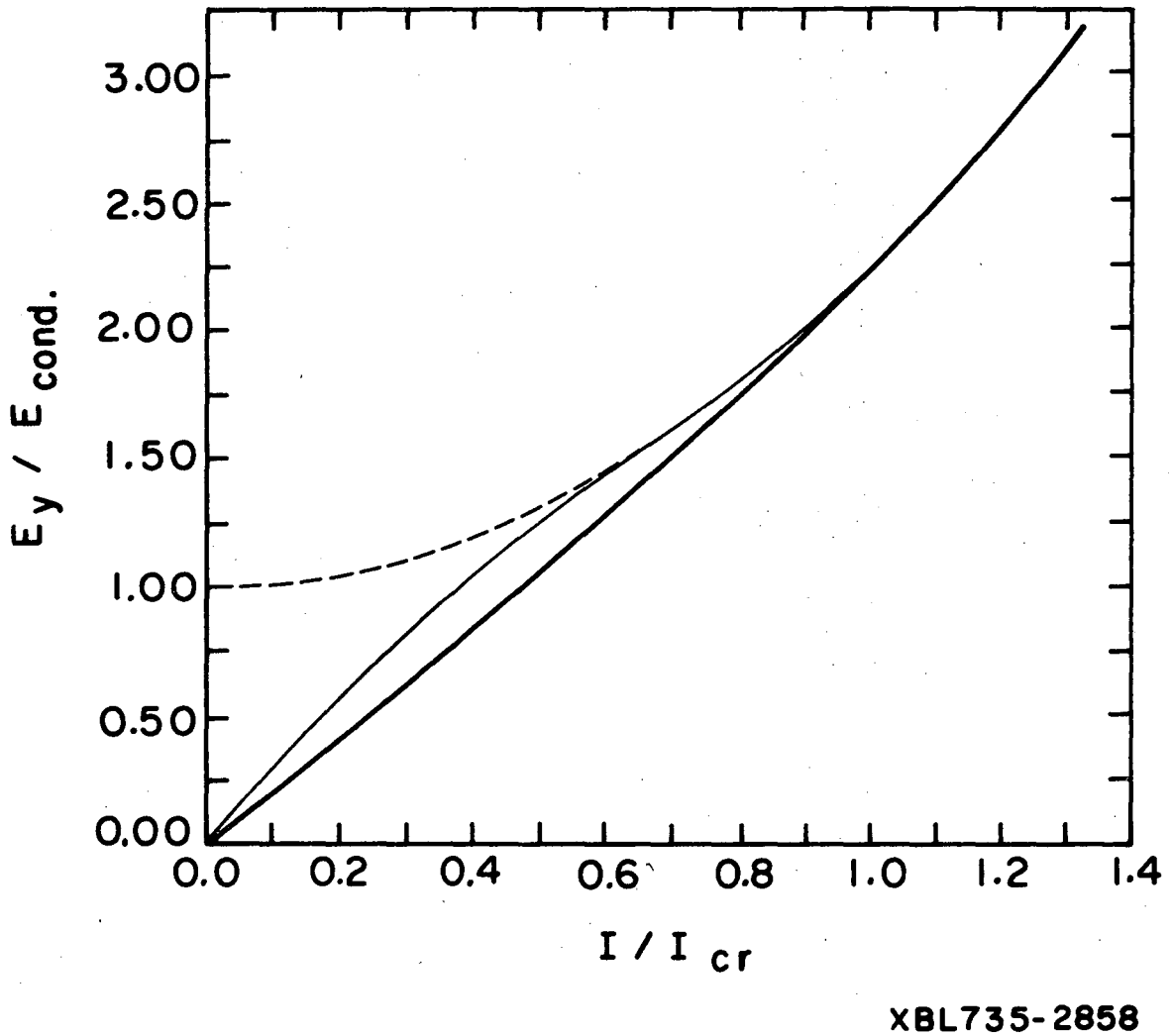

XBL735-2858

Fig. 3

LEGAL NOTICE

This report was prepared as an account of work sponsored by the United States Government. Neither the United States nor the United States Atomic Energy Commission, nor any of their employees, nor any of their contractors, subcontractors, or their employees, makes any warranty, express or implied, or assumes any legal liability or responsibility for the accuracy, completeness or usefulness of any information, apparatus, product or process disclosed, or represents that its use would not infringe privately owned rights.

TECHNICAL INFORMATION DIVISION
LAWRENCE BERKELEY LABORATORY
UNIVERSITY OF CALIFORNIA
BERKELEY, CALIFORNIA 94720